Thermodynamics of Single Strand DNA Base Stacking

Jayanthi Ramprakash, Brian Lang, Frederick P. Schwarz
Center for Advanced Research in Biotechnology, National Institute of Standards and Technology, 9600 Gudelsky Drive, Rockville, MD 20850

Received 13 May 2008; revised 12 June 2008; accepted 17 June 2008
Published online 8 July 2008 in Wiley InterScience (www.interscience.wiley.com). DOI 10.1002/bip.21044

ABSTRACT:

The thermodynamics of the stacking to unstacking transitions of 24 single-stranded DNA sequences (ssDNA), 10–12 bases in length, in sodium phosphate buffer were determined from 10 to 95°C, using differential scanning calorimetry (DSC). An additional 22 ssDNA sequences did not exhibit an S⇔U transition in this temperature range. The transition properties of the ssDNA sequences with ≤60% self-complementarily in the reverse direction were independent of concentration with transition temperatures ranging from 15 to 70°C, van't Hoff transition enthalpies from 92 to 201 kJ mol^{-1} and transition enthalpies from 5 to 75% of the corresponding van't Hoff transition enthalpies. Since all the 16 doublets and 60 of the 64 triplets are present in both the transition and the non-transition ssDNA sequences, it is unlikely that the nucleation subset initiating stacking of the sequence is a specific doublet or triplet subset. Of the 141 quadruplet subsets of the 46 sequences, each transition ssDNA sequence contained at least one or more quadruplets not found in the non-transition ssDNA sequences. It could be concluded that the thermal stability of the stacked conformation was dependent on the presence of a possible nucleation quadruplet and the length of the ssDNA sequence and not on the G or C content of the ssDNA sequence, nor on the number of purine bases in the sequence. © *2008 Wiley Periodicals, Inc.*† *Biopolymers 89: 969–979, 2008.*

Keywords: differential scanning calorimetry; single strand DNA; stacking transitions; thermodynamics; transition enthalpy; transition temperature

This article was originally published online as an accepted preprint. The "Published Online" date corresponds to the preprint version. You can request a copy of the preprint by emailing the Biopolymers editorial office at biopolymers@wiley.com

INTRODUCTION

Investigations of many of the biological processes involving single-stranded DNA (ssDNA) often focus exclusively on the thermodynamic role of the protein and not on any thermodynamic role of the ssDNA base stacking conformation in these processes. The stacking of the bases of ssDNA was first investigated in the 1960s by monitoring the spectral shift in the UV absorption spectra of the nucleotides with increase in temperature similar to that observed for UV melting scans of DNA duplexes. Since then, additional methods, such as optical rotary dispersion[1] and calorimetry,[2,3] have been employed to investigate ssDNA stacking. The nature of the stacking to unstacking (S⇔U) transition of a specific ssDNA, 5′-ATGCTGATGC-3′, has more recently been confirmed by small angle neutron scattering[4] (SANS) in addition to differential scanning calorimetry[3] (DSC) and UV melting measurements.

Cylindrical, helical, and random coil shape models of 5′-ATGCTGATGC-3′ fitted to the SANS measurements at each temperature exhibited an expansion in the diameter direction causing a slightly shortened pitch from 25 to 43°C, an expansion in the pitch direction with a slight decrease in the diameter from 43 to 53°C, and finally a dramatic increase in the pitch and diameter from 53 to 80°C. Analysis of the DSC

Correspondence to: F. P. Schwarz; e-mail: fred@carb.nist.gov

scans of the sequence in solution over a concentration range from 0.12 to 1.29 m*M* exhibited a reversible two-state transition profile with a transition temperature of 47.5°C ± 0.5°C, the mid point of the conformational changes observed in the SANS measurements, a van't Hoff enthalpy of 93 ± 5 kJ mol^{-1}, and a calorimetric transition enthalpy of 60 ± 3 kJ mol^{-1} independent of concentration that indicates a broad transition as is observed in the SANS measurements.[4]

Interestingly, the ratio would be the same if only two pair-wise interactions out of the total possible nine pair-wise interactions between two adjacent nucleotide bases was responsible for the calorimetric enthalpy of the 10mer ssDNA sequence. Similar results also were observed earlier for RNA sequences where the transition van't Hoff enthalpy derived from the UV melting curves was independent of chain length in going from the dinucleoside ApA to a longer poly A sequence.[5] More importantly, the stacking of the nucleotides in ssDNA over this temperature range has been shown to be responsible for the disparity between the results of calorimetry measurements on the association of complementary ssDNA strands at ambient temperatures and the results extrapolated from dissociation of the DNA duplexes performed at high temperatures or melting of the duplex.[2,6] This disparity resulted from the initial states of the ssDNA at ambient temperatures being in the stacked conformation, whereas the final states of the dissociated ssDNA strands at high temperature are in a random coil conformation. Similar disparities between DSC measurements on the dissociation of 10–16 bp DNA duplexes and ITC measurements on the formation of the duplexes have also suggested a role for enthalpy contributions from residual structure in the ssDNA strands.[7] It is not known if or how the thermal stability of the stacked conformation is dependent on the ssDNA sequence or how the stacking of the bases is initiated. For example, the nearest neighbor model for predicting DNA duplex stability from the duplex sequence is based on assigning thermodynamic values to adjacent dinucleotide subsets and a similar model may apply to predicting the thermodynamic stability of the stacked ssDNA sequences. The stacking of bases is presumed to be initiated by a nucleation site consisting of stacked two or more adjacent bases followed by stacking of the entire ssDNA sequence.

A more recent study[8] suggested that the nucleation site for single strand stacking may be a triplet set of nucleotides and there are a total of 64 different triplets of the four nucleotides. It is also not known how the stacking conformation of ssDNA thermodynamically affects many of the biologically processes that involve ssDNA. For example, transcription of a gene by RNA polymerase is initiated by separation of the bases upstream from the transcription start point on the promoter into its complementary single strand sequences to form a "transcription bubble" just prior to transcription into messenger RNA. Furthermore, many of the biological processes involving ssDNA are also dependent on the directionality of the phosphodiester backbone of the sequence. For example, transcription of promoters into RNA and subsequent elongation of the RNA proceeds in the 5′ to 3′ direction on the RNA and, thus, the complementary single DNA strand is being transcribed in the 3′ to 5′ direction.

The goals of this investigation was to further investigate the two-state S⇔U nature of the transition as a function of ssDNA sequence, to determine the dependence of the stability of the stacked conformation on the sequence, and to determine the size of the nucleation subset responsible for initiation of the stacking conformation. DSC scans were performed on 36 different ssDNA sequences, ranging in length from 10 to 12 bases, between 10 and 95°C, a temperature range 10°C above the freezing point of water and 5°C below the boiling point of water. Fourteen of the ssDNA strands did not exhibit a detectable transition in this temperature range. The transition peak areas of the remaining 22 ssDNA sequences ranged from a barely detectable 1 to100 kJ mol^{-1}. DSC scans were also performed over almost an order of magnitude of ssDNA concentration for the ssDNA sequences exhibiting transition peak areas enthalpies greater than 20 kJ mol^{-1}. A simple A⇔B transition model was then employed to analyze the S⇔U transitions of those sequences that exhibited transition temperature maxima independent of the ssDNA concentration. The investigation was extended to include an additional 10 ssDNA promoter sequences that comprise most of the RNA polymerase initiation transcription "bubble" in *E. coli* to determine if the stacking stabilities of the ssDNA sequences have any correlation with the lifetime of the initial transcription bubble–RNA polymerase complex formed from these promoters. The lifetimes of these initiation complexes range from 7.5 to 270 min depending on the sequence of the promoter.[9] All the ssDNA sequences contained the 16 doublet and 64 triplet combinations of the four bases in the 5′ to 3′ direction and were non-palindromic sequences to avoid any loop formation of the ssDNA sequence. The lack and presence of an S⇔U transition was determined as a function of the presence of a specific doublet, triplet, or quadruplet sequence in the ssDNA sequence.

MATERIALS AND METHODS

Materials

The lyophilized synthetic ssDNA sequences were obtained from two sources, Oligos, etc. and Integrated DNA Technologies, as de-salted

and HPLC purified and used without any further purification. The sodium mono and dibasic phosphates, EDTA, and sodium chloride were obtained as reagent grade from Sigma-Aldrich. The solutions were prepared by adding the appropriate volume of 10 m*M* sodium phosphate +1 m*M* EDTA at pH = 7.0 buffer to the sample vial containing the desalted, lyophilized DNA. The solution was vortexed to ensure dissolution of all the ssDNA in the sample vial and the solution was stored at −20°C until use. The concentration of the ssDNA was determined by UV absorption measurements at 260 nm and use of the extinction coefficients from the supplier or from Ref. 10.

Differential Scanning Calorimetry

DSC measurements were performed on 0.2–3 m*M* solutions of the ssDNA employing a VP-DSC Microcalorimeter from Microcal (Northampton, MA). The DSC consists of a matched pair of 0.511 mL sample and reference vessels. In a series of DSC scans, both vessels were first loaded with buffer solution, equilibrated at 5°C for 15 min. scanned up to 95°C at a pre-set scan rate of 60°C h^{-1}. The buffer versus buffer scan was repeated once for a second scan following cooling of the first scan. After cooling of the second scan, the sample vessel was then emptied and loaded with the DNA solution by means of a syringe and prior to the 15 min. equilibration period at 5°C. The scan was repeated several times to verify the reversibility of the transition. After completion of a set of scans, a buffer versus buffer scan was used as the baseline scan and subtracted from each of the DNA solution versus buffer scans prior to analysis. The net DNA solution versus buffer scan was converted to a heat capacity versus temperature scan and, with the one exception of a transition that exhibited a dependence of the transition temperature maximum on concentration, all the transitions were analyzed in terms of a A⇔B two-state thermodynamic transition model, using the EXAM software program.[11] Any transition that exhibited a dependence of its temperature maximum on concentration was analyzed in terms of a A⇔2B transition model, using the EXAM program.[11] The EXAM program[11] determines the transition peak area, the transition van't Hoff enthalpy ($\Delta_{trs}H_{vH}$), and the temperature (T_m) where the transition peak area is half of the total area. The transition van't Hoff enthalpy is determined from $d(\ln\{K(T)\})/d(1/T)$ where the transition equilibrium constant, $K(T)$ is determined from the fractional area, $\alpha(T)$ up to a temperature T. The ratio of the transition peak area to the amount of DNA in the sample vessel yielded values for the transition enthalpy ($\Delta_{trs}H$). DSC scans were performed on different concentrations of each ssDNA sequence exhibiting a transition enthalpy $\geq$20 kJ mol^{-1} either in the 0.1*M* NaCl or non NaCl buffers to determine any dependence of the transition properties on concentration. Low concentrations of ssDNA sequences with transition enthalpies below 20 kJ mol^{-1} were too difficult to analyze precisely, particularly over an order of magnitude in concentration. The uncertainties in T_m and the van't Hoff transition enthalpies, and transition enthalpies were determined as a standard deviation of the average value of different DSC scans of the samples.

Optical Density Measurements

To verify the lack of an S⇔U transition of a specific ssDNA sequence in the temperature range from 10 to 95°C, optical density (OD) measurements at 260 nm were performed on the sequences at 10 and at 85°C. A transition from the hydrophobic environment of the bases in a stacked position to an aqueous environment of the unstacked bases produces an increase in the OD of the solution and is the basis of the UV melting method. A lack of a transition would result in almost no change in the OD over this temperature range. The OD measurements were performed by a Perkin–Elmer Lambda 4B Spectrophotometer, and the temperature of the optical cell was maintained by PTP-1 Peltier Temperature Controller interfaced with the spectrophotometer. The measurements were performed on samples of the same ssDNA solutions at 10°C, then at 85°C, and finally at 10°C again. As a control, OD measurements were also performed on some of the sequences exhibiting a transition within this range.

Determination of the Triplet and Quadruplet Subsets in the ssDNA

The triplet subsets of an ssDNA were determined by starting with the first nucleotide at the 5′ end and listing this nucleotide as the first nucleotide of the triplet subset and then starting with the next nucleotide listing it as the first nucleotide of the second triplet subset of the ssDNA sequence. The last triplet subset of the sequence includes the last nucleotide at the 3′ end. For example, GTGCTTTGTATC breaks down into the triplet subsets GTG, TGC, GCT, CTT, TTT, TTG, TGT, GTA, TAT, and ATC. Although the triplet subsets contained nucleotides from other subsets in the sequence, this method was employed because it was not certain, which adjacent nucleotides formed the specific subset responsible for nucleation of the entire sequence. In a similar method, the quadruplet subsets of GTGCTTTGTATC were determined as GTGC, TGCT, GCTT, CTTT, TTTG, TTGT, TGTA, GTAT, and TATC.

RESULTS

The results of typical DSC scans of two 10mer ssDNA sequences (8 and 22 in Table I) are presented in Figure 1. (The sequences are numbered in the tables for reference in the text.) Although the difference in the two sequences is only a change of the two central bases from AG for the low temperature transition to GT for the high temperature transition in Figure 1, the transition temperature is almost 20 degrees higher for the high temperature transition. Since both sequences exhibited transition temperature maxima independent of concentration, 0.67–1.1 m*M* for ssDNA sequence 8 and 0.10–1.27 m*M* for ssDNA sequence 22 in 0.1*M* NaCl buffer, a two-state A⇔B transition model was fitted to the heat capacity data for the ssDNA S⇔U transitions as shown specifically for ssDNA sequence 8 (5′ATGCAGATGC3′) in Figure 2 and the parameters for this fit are presented in Table I. It should be noted that the transition temperature determined for two-state A⇔B transitions is the same as the temperature at the transition peak maximum for transitions exhibiting small changes in the heat capacity between the initial A state and the final B state. It was found that ssDNA sequence 5 (5′CGTACATGTA3′) with 80% of its bases self-complementary in the reverse direction,

Table I Thermodynamic Parameters of the S⇔U Transition of ssDNA Sequences from Fits of a Two-State Transition Model to the DSC Results

Sequence	[NaCl] (*M*)	[ssDNA] (m*M*)	T_m (°C)	$\Delta_{trs}H_{vH}$ (kJ mol^{-1})	$\Delta_{trs}H$ (kJ mol^{-1})	$\Delta_{trs}H/\Delta_{trs}H_{vH}$
1. ACCATTATGT	0	2.10	15.0 ± 0.5			
	0.10	1.05	20.8 ± 0.1	184 ± 1	25.0 ± 0.4	0.14 ± 0.01
2. GTGCTTTGTATC	0	1.81	19.2 ± 0.1	134 ± 2	22 ± 1	0.16 ± 0.02
	0.10	0.81		transition shifted to lower temperature		
3. TAATACATGC	0	2.28	19.4 ± 0.1	131 ± 1	7.1 ± 0.3	0.05 ± 0.02
	0.10	1.14	24.5 ± 0.3	127 ± 4	13.6 ± 0.9	0.11 ± 0.01
4. CCATTTGTGA	0	0.54	24.6 ± 0.6	131 ± 4	16.5 ± 0.8	0.13 ± 0.01
	0.10	0.27	23.5 ± 0.7	145 ± 1	10 ± 1	0.07 ± 0.01
5.*CGTACATGTA*[a]	0	0.125–0.84	22.8–36.0	263 ± 6	134 ± 23	0.51 ± 0.09
	0.10	0.23	36.4 ± 0.4	279 ± 3	113 ± 3	0.41 ± 0.01
6. GATACTGAGCGT	0	0.26–2.17	29.4 ± 1.0	136 ± 20	41 ± 1	0.35 ± 0.01
	0.10	0.95	37.4 ± 0.1	156 ± 1	24 ± 1	0.15 ± 0.01
7. CACATTTGTA	0	4.82	32.5 ± 0.2	126 ± 4	6.7 ± 0.9	0.05 ± 0.01
	0.10	2.41	34.5 ± 0.6	168 ± 9	1.2 ± 0.1	0.010 ± 0.001
8. ATGCAGATGC	0	0.42	37.1 ± 0.2	201 ± 3	14 ± 1	0.07 ± 0.01
	0.10	0.67–1.1	47.0 ± 1.5	175 ± 6	16 ± 2	0.09 ± 0.01
9. CGTGCGTACAC	0	0.30–2.84	38.7 ± 1.1	121 ± 10	55 ± 3	0.45 ± 0.05
	0.10	1.42	41.1 ± 0.1	131 ± 3	59 ± 4	0.45 ± 0.03
10. ATGCCGATGC	0	0.24–1.38	40.0 ± 3.4	99 ± 13	14 ± 1	0.14 ± 0.02
	0.10	0.46	47.0 ± 1.2	92 ± 2	37 ± 5	0.40 ± 0.05
11. TATGCAGATGCT	0	0.29–2.04	40.6 ± 2.2	145 ± 4	52 ± 5	0.36 ± 0.03
	0.10	0.27	42.2 ± 1.7	125 ± 10	22 ± 4	0.18 ± 0.03
12. ATGCTCCATGC	0	1.18	43.8 ± 0.1	103 ± 1	12 ± 1	0.12 ± 0.01
	0.10	1.16	44.8 ± 0.1	110 ± 1	7.9 ± 0.4	0.072 ± 0.004
13. ATGCCCATGC	0	0.52	44.1 ± 2.4	107 ± 14	12 ± 4	0.11 ± 0.04
	0.10	1.48	44.8 ± 1.0	98 ± 8	10.7 ± 0.5	0.13 ± 0.02
14. GCATAGGCAT	0	0.24–0.93	44.6 ± 2.2	130 ± 16	17 ± 2	0.26 ± 0.04
	0.15	1.02	34.3 ± 0.2	137 ± 10	35 ± 5	0.38 ± 0.08
	0.30	0.78	37.7 ± 0.2	137 ± 11	52 ± 8	0.38 ± 0.08
15. ATGCTGATGC	0	0.21	46.1 ± 0.5	92 ± 5	33 ± 2	0.36 ± 0.03
	0.10	0.12–1.3	47.5 ± 0.3	95 ± 5	32 ± 3	0.34 ± 0.04
16. ATGCCTATGC	0	0.51–1.22	46.1 ± 0.3	114 ± 6	16 ± 2	0.14 ± 0.02
	0.10	0.19–0.24	48.9 ± 0.8	130 ± 27	7 ± 1	0.054 ± 0.008
	0.15	1.14	49.5 ± 0.7	107 ± 4	26 ± 4	0.24 ± 0.04
	0.30	1.34	51.7 ± 0.3	112 ± 3	16 ± 2	0.14 ± 0.02
17. GCATACGCAT	0	0.212–1.66	48.4 ± 2.4	110 ± 7	51 ± 2	0.46 ± 0.04
	0.10	1.16	50.0 ± 1.5	121 ± 1	79.3 ± 0.5	0.66 ± 0.04
18. GCATCGGCAT	0	0.207–0.817	48.0 ± 1.6	110 ± 8	26 ± 5	0.24 ± 0.05
	0.10	0.39	47.0 ± 1.6	92 ± 2	54 ± 4.0	0.59 ± 0.04
19. ATGCAAATGC	0	0.88	48.1 ± 0.4	98 ± 1	25 ± 1	0.26 ± 0.01
	0.10	0.27–0.79	45.9 ± 0.3	109 ± 23	59 ± 14	0.54 ± 0.17
	0.15	0.84	50.1 ± 1.9	108 ± 12	17 ± 4	0.16 ± 0.04
	0.30	1.59	51.3 ± 0.8	102 ± 3	17 ± 3	0.16 ± 0.02
20. GCATGTGCAT	0	0.51–1.23	48.8 ± 0.7	142 ± 21	37 ± 3	0.26 ± 0.04
	0.10	0.19	36.8 ± 0.1	121 ± 15	17 ± 1	0.14 ± 0.02
	0.15	1.04	44.1 ± 0.6	141 ± 7	86 ± 11	0.61 ± 0.08
	0.30	1.12	47.0 ± 0.1	143 ± 1	103 ± 1	0.72 ± 0.01
21. GCATTTGCAT	0	0.141–0.811	48.5 ± 2.2	128 ± 12	72 ± 1	0.56 ± 0.05
	0.10	1.08	47.5 ± 0.7	119 ± 6	5.9 ± 0.3	0.050 ± 0.004
22. ATGCGTATGC	0	0.19–0.96	69.9 ± 0.6	127 ± 10	68 ± 10	0.54 ± 0.09
	0.10	0.10–1.27	69.8 ± 1.0	188 ± 17	44 ± 2	0.24 ± 0.02
	0.15	0.96	69.8 ± 0.3	141 ± 7	70 ± 27	0.50 ± 0.19
	0.30	1.10	70.0 ± 0.7	123 ± 9	69 ± 7	0.56 ± 0.06

[a] Only ssDNA sequence analyzed in terms of a A⇔2B dissociative transition model.

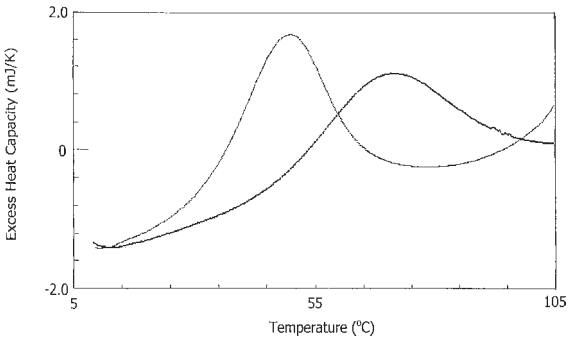

FIGURE 1 DSC scans of 1.1 m*M* 5′ATGCAGATGC 3′, sequence 8 in the text, (lower temperature transition) and 1.3 m*M* 5′ATGCGTATGC 3′, sequence 22 in the text, (higher temperature transition) in 10 m*M* sodium phosphate +1 m*M* EDTA +0.1*M* sodium chloride buffer (pH = 7.0) at 60°C h^{-1}.

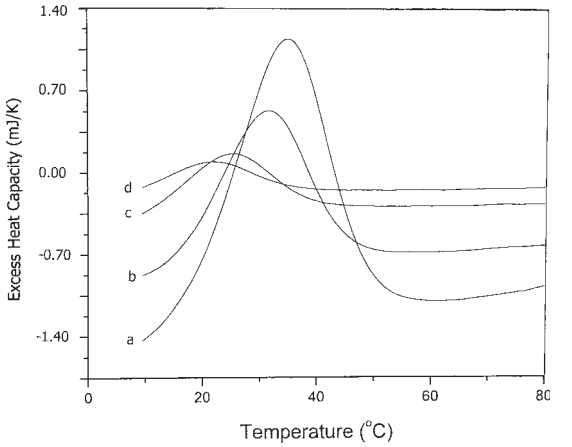

FIGURE 3 Results of DSC scans on 5′CGTACATGTA3′ in 10 m*M* sodium phosphate +1 m*M* EDTA buffer (pH = 7.0) at concentrations of 0.814 m*M* (a), 0.476 m*M* (b), 0.217 m*M* (c), and 0.125 m*M* (d) at 60°C h^{-1}.

however, exhibited a dependence of the transition temperature maxima on concentration as shown in Figure 3, and was, thus, analyzed in terms of a dissociative A⇔2B transition model, as shown in Figures 4 and 5.

The lack of a transition temperature maximum dependence on concentration for the other ssDNA sequences is shown typically in Figure 6 for ssDNA sequence 9 (5′CGTGCGTACAC3′), which has only 60% of its bases self-complementary in the reverse direction. It should be noted that despite almost the same transition temperatures of ssDNA sequences 5 and 9, the nature of their transitions is different. Since the remaining 45 ssDNA sequences had only 40–60% of their bases self-complementary in the reverse direction, including those ssDNA sequences in Tables II and III not exhibiting a detectable transition from 10 to 95°C, the remaining transitions were consistently analyzed in terms of a A⇔B two-state transition model. The fitting thermodynamic parameters for the transitions of 20 additional ssDNA sequences in 0 and 0.1*M* NaCl are presented in Table I, including the 14 ssDNA sequences with transition enthalpies ≥20 kJ mol^{-1}, which were determined over a range of concentrations.

DSC scans of the 14 ssDNA sequences listed in Table II and the 7 ssDNA sequences in Table III resulted in straight lines without any evidence of a transition from 10 to 95°C, as typically shown in Figure 7. A S⇔U transition in this temperature range would also result in an increase in the OD at 260 nm[4,6] as also shown for ssDNA sequences 37, 41, and 42 in 0.1*M* NaCl buffer in Table III. The lack of an S⇔U transition for any of the 14 ssDNA sequences listed in Tables II was further substantiated by the unity of their 85–10°C OD ratios at 260 nm with the one exception of ssDNA 35 in Table II. Although DSC scans of ssDNA sequence 35 do not exhibit

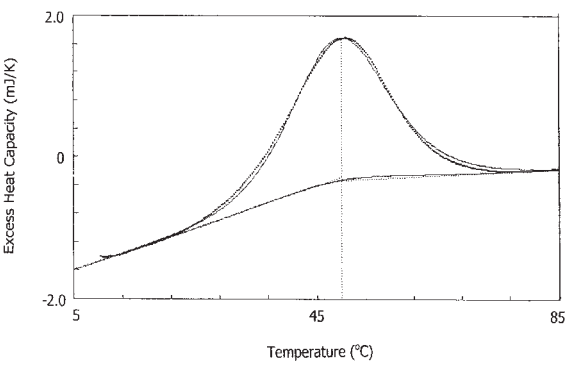

FIGURE 2 Least squares fit of a two-state A⇔B transition model along with the interpolated baselines to the DSC data of the1.1 m*M* 5′ATGCAGATGC3′ strand transition in 10 m*M* sodium phosphate +1 m*M* EDTA +0.1*M* sodium chloride buffer (pH = 7.0) at 60°C h^{-1}exhibited in Figure 1.

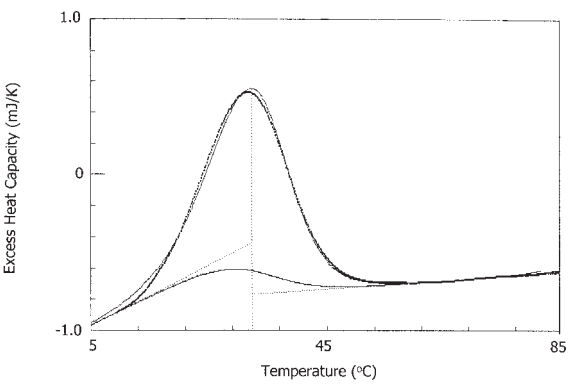

FIGURE 4 Least squares fit of a two-state A⇔2B transition model along with the interpolated baselines to the DSC data of the 0.476 m*M* 5′CGTACATGTA3′ strand transition in 10 m*M* sodium phosphate +1 m*M* EDTA (pH = 7.0) at 60°C h^{-1}exhibited by curve (b) in Figure 3.

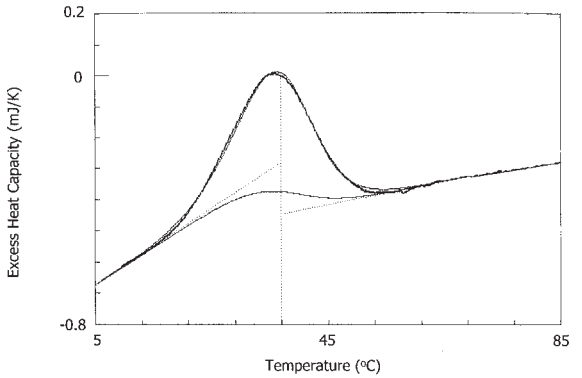

FIGURE 5 Least squares fit of a two-state A⇔2B transition model along with the interpolated baselines to the DSC data of the 1.42 m*M* 5′CGTACATGTA3′ strand transition in 10 m*M* sodium phosphate +1 m*M* EDTA (pH = 7.0) + 0.1*M* sodium chloride at 60°C h^{-1}.

any transition, it is not known as why this sequence exhibits a ratio of 1.09 ± 0.01, almost the same as for sequences undergoing an S⇔U transition listed in Table III. Shorter 8mer and 9mer ssDNA sequences of the sequences listed in Table I also did not exhibit any evidence for a transition from 10 to 95°C. The transition temperatures range from 15°C for ssDNA sequence 1 to 70°C for ssDNA sequence 22 in the absence of salt with most of the transition temperatures in the range from 39 to 50°C. Similarly, the van't Hoff enthalpies range from 92 kJ mol^{-1} for ssDNA sequence 15 in the absence of NaCl, and ssDNA sequences 10 and 18 in 0.1*M* NaCl to 201 kJ mol^{-1} for ssDNA sequence 8 in the absence of salt with the all the van't Hoff enthalpies averaging 123 kJ mol^{-1} in the absence of NaCl and 134 kJ mol^{-1} in the presence of 0.1*M* NaCl.

All the calorimetric enthalpies calculated from the observed transition enthalpies are less than the van't Hoff enthalpies, perhaps because the calorimetric enthalpies are difficult to determine accurately over the large temperature ranges of the transitions and the baseline under the transition peak is an intrapolation from the pre and post-transition baselines. For example, if a straight baseline is extrapolated between the temperature of the transition onset and the temperature of the return of the transition to the post-transitional baseline in Figures 4 and 5, then the calorimetric transition enthalpies would increase by 17–20%, while reducing the closeness of the fit to the DSC data, and while still keeping the transition enthalpy ratios below unity.

In DSC practice, a straight baseline over a temperature range of 39°C even for buffer versus buffer scans does not occur so a straight baseline extrapolated under the transition peak would not be appropriate. Instead an extrapolated sigmoidal baseline following the profile of the transition peak was employed. More specifically, the transition enthalpy to the van't Hoff transition enthalpy ratios range from a low of 0.010 ± 0.001 for ssDNA sequence 7 in 0.10*M* NaCl to 0.75 ± 0.03 for ssDNA sequence 20 0.3*M* NaCl yielding an average value for all the sequences of 0.27 in the absence of NaCl and 0.24 in the presence of 0.10*M* NaCl. Alternatively the transitions may be classified into weak transitions with an average transition enthalpy to van't Hoff transition enthalpy ratio ≤0.10 for ssDNA sequences 1–4, 7, 8, 12, 13, and 16 and strong transitions with an average ratio of 0.36 for ssDNA sequences 5, 6, 9–11, 14, 15, and 17–22. At 0.1*M* NaCl, most of the ssDNA sequences in Table I exhibited an increase in the transition temperature with the exception of ssDNA sequences 4, 13, 14, and 18–22. In contrast, the ssDNA sequences 4, 14, 20, and 21 exhibited a decrease in T_m at 0.1*M* NaCl, whereas ssDNA sequences 13, 18, and 22 did not exhibit any change in T_m in the presence of NaCl. Since an increase from 0.1 to 0.3*M* NaCl has no additional affect on the transition properties for ssDNA sequences 19, 20, and 22, the affect of NaCl on the transition temperatures appears to saturate at 0.1*M* NaCl.

To determine any effect of the stacking stability (lifetime) of the initial promoter-RNA polymerase transcription initiation complex, DSC scans were performed on the ssDNA sequences of 10 promoters sequenced from the transcription start point to and including the TATA box sequence centered at −10. (The transcription bubble usually includes bases from the center of the TATA box to and just downstream from the transcription start point.) Typical DSC scans of the promoter ssDNA sequences are shown in Figure 7, where ssDNA sequences 41 (5′TATAATGGTACC3′) and 37 (5′TATAATGTGTGG3′) exhibit S⇔U transitions, whereas ssDNA sequence 45 (5′GACAATAACCCT3′) does not exhibit a transition. The ssDNA sequences 37, 38, and 41 have only

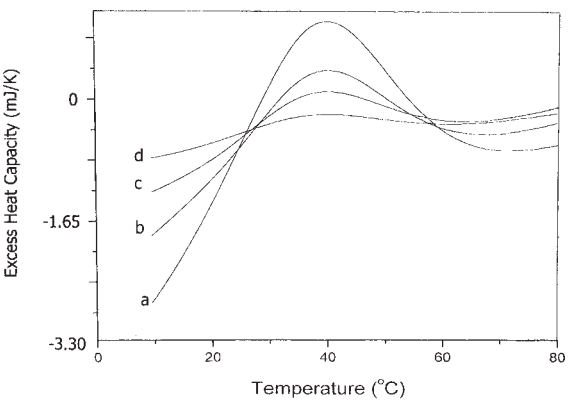

FIGURE 6 Results of DSC scans on 5′CGTGCGTACAC3′ in 10 m*M* sodium phosphate +1 m*M* EDTA buffer (pH = 7.0) at concentrations of 1.98 m*M* (a), 1.18 m*M* (b), 0.756 m*M* (c), and 0.226 m*M* (d) at 60°C h^{-1}.

Table II ssDNA Sequences Not Undergoing a S⇔U Transition from 10 to 95°C

Sequence	[NaCl] (*M*)	[DNA] (m*M*)	OD (85°C)/ OD (10°C)
23. ATGCCGAATGC	0	1.84	1.00 ± 0.01[a]
24. ATGCCTTATGC	0	0.95	1.00 ± 0.01[a]
25. ATGCAAGATGC	0	0.87	1.02 ± 0.01[a]
26. ATGCGGTATGC	0	1.10	1.04 ± 0.01[a]
27. ATGCGGAATGC	0	0.82	1.02 ± 0.01[a]
28. CCACGTATTATA	0	1.42	0.92 ± 0.01
29. CCGTACATTATA	0	1.73	1.01 ± 0.01
30. CCATTTATTATA	0	0.97	1.06 ± 0.01[a]
31. GATACTCGTCAC	0	1.68	0.97 ± 0.01
32. GATCGTGAGCAC	0	1.80	0.99 ± 0.01[a]
33. GATACTTTTCAC	0	1.77	0.99 ± 0.01
34. GGTGCCGTGTATC	0	1.72	1.01 ± 0.01
35. AGGCAATACT	0, 0.1	3.94	1.09 ± 0.01
36. CATTGCCTTA	0	1.36–5.77	1.05 ± 0.01

[a] OD measurements were in 0.1*M* NaCl buffer.

33% of their bases self-complementary in the reverse direction, while ssDNA sequence 42 has 50% of its bases self-complementary in the reverse direction. The thermodynamic parameters describing the S⇔U transitions of ssDNA sequences 37, 38, 41, and 42 from 10 to 95°C are presented in Table III.

Promoter sequences 38, 40, 42, 44, and 46 are complements, respectively, of the promoter sequences 37, 39, 41, 43, and 45. The promoters designated P_{N25} and $P_{N25/O3}$ have the same transcription bubble sequences 43 and 44 as do the P_{tac} and P_{LUV5} promoters with transcription bubble sequences 37 and 38.[9] These promoters with the same bubble sequences have the same initial RNA polymerase–promoter transcription complex lifetimes of 180 min for P_{N25} and $P_{N25/O3}$ and 10–7.5 min for P_{tac} and P_{LUV5}.[9] Only three of the seven promoter transcription bubble sequences investigated exhibit a S⇔U transition in the temperature range from 10 to 95°C. The sequences of the P_{tac} and P_{LUV5} promoters exhibit transitions from 25 to 29°C and the sequences of the P_{con} promoter exhibit transitions from 32 to 40°C. Similar to that observed for sequences 1–21 in Table I, the sequences of these promoters exhibit transitions with van't Hoff enthalpies ranging from 97 to 224 kJ mol^{-1} and lower transition enthalpy to van't Hoff enthalpy ratios of 0.08–0.55 for the sequences. There is an increase in the transition temperature of the ssDNA promoter sequences but not necessarily an increase in the van't Hoff enthalpy, in the presence of 0.1*M* NaCl. There does not seem to be any correlation between the lifetimes of the initiation complexes and the presence of an S⇔U transition in the ssDNA sequence. The absence of a S⇔U transition in those promoter sequences 38, 39, 40, and 43–46 was further substantiated by the near unity OD ratios of OD (85°C)/OD (10°C) as shown in Table III in contrast to the corresponding ratios of ∼ 1.10 for transition ssDNA sequences 37, 41, and 42 as shown in Table III.

Table III Thermodynamic Parameters of the S⇔U Transition of Transcription "Bubble" Sequences of Promoters from Fits of a Two-State Transition Model to DSC Results

Promoter Sequence (Name)	[P] (m*M*)	$t_{1/2}$ (min)	[NaCl] (*M*)	T_m (°C)	$\Delta_{trs}H_{vh}$ (kJ mol^{-1})	$\Delta_{trs}H$ (kJ mol^{-1})	$\Delta_{trs}H/\Delta_{trs}H_{vh}$ (85/10)	OD
P_{tac} and P_{LUV5} Promoters:								
37. TATAATGTGTGG	1.77	10, 7.5	0	25.0 ± 1.2	97 ± 2	53 ± 1	0.55 ± 0.01	
	0.81	10, 7.5	0.10	29.4 ± 1.0	138 ± 11	41 ± 4	0.30 ± 0.04	1.07 ± 0.01
38. CCACACATTATA	1.33	10, 7.5	0		No transition			1.00 ± 0.01
P_L Promoter:								
39. GATACTGAGCAC	1.73	17	0		No transition			1.01 ± 0.01
40. GTGCTCAGTATC	1.92	17	0		No transition			1.01 ± 0.01
P_{con} Promoter:								
41. TATAATGGTACC	1.79	84	0	32.8 ± 0.1	148 ± 4	49 ± 4	0.33 ± 0.03	
	0.95	84	0.10	39.9 ± 1.2	224 ± 11	18 ± 2	0.08 ± 0.01	1.09 ± 0.01
42. GGTACCATTATA	2.78	84	0	26.8 ± 0.6	152 ± 4	47 ± 2	0.31 ± 0.01	
	1.40	84	0.10	43.2 ± 0.3	151 ± 4	50 ± 1	0.33 ± 0.01	1.11 ± 0.01
P_{N25} and $P_{N25/O3}$ Promoters:								
43. TATAATAGATTC	2.00	180	0		No transition			1.01 ± 0.01
44. GAATCTATTATA	2.84	180	0		No transition			1.01 ± 0.01
P_{bla} Promoter:								
45. GACAATAACCCT	1.95	270	0		No transition			1.01 ± 0.01
46. AGGGTTATTGTC	1.68	270	0		No transition			1.00 ± 0.01

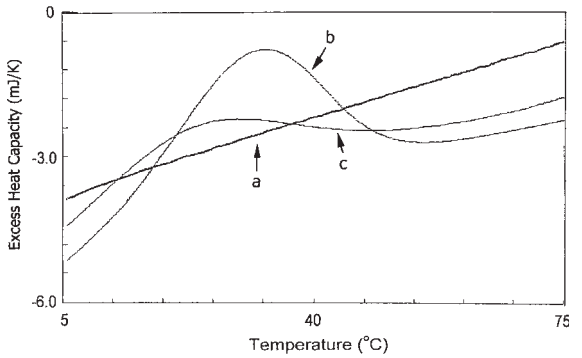

FIGURE 7 Results of DSC scans on ssDNA sequences of the transcription bubbles of various promoters; (a) DSC scan of 1.9 m*M* 5′GACAATAACCCT3′, sequence 45 in the text, in 10 m*M* sodium phosphate +1 m*M* EDTA +0.1*M* sodium chloride buffer (pH = 7.0) at 60°C h^{-1}, (b) DSC scan of 1.8 m*M* 5′TATAATGGTACC3′, sequence 41 in the text, in 10 m*M* sodium phosphate +1 m*M* EDTA +0.1*M* sodium chloride buffer (pH = 7.0) at 60°C h^{-1}, and (c) DSC scan of 1.5 m*M* 5′TATAATGTGTGG3′ (Sequence 37) in 10 m*M* sodium phosphate +1 m*M* EDTA +0.1*M* sodium chloride buffer (pH = 7.0) at 60°C h^{-1}.

DISCUSSION

SANS results on the stacking transition of sequence 15 (5′-ATGCTGATGC-3′) in an earlier report[4]do show stacking of the entire ssDNA sequence at low temperature and unstacking at high temperature, as well as independence of the transition temperature on the ssDNA concentration. Accordingly, the transitions were analyzed in terms of a simple A⇔B transition model. There is the possibility that the observed transitions of the sequences in Tables I and III could result from dissociation of a dimer of the sequence, as shown by ssDNA sequence 5 in Table I,

$$\begin{matrix} 5'\ \mathrm{CGTACATGTA}\ 3' \\ 3'\ \mathrm{ATGTACATGC}\ 5' \end{matrix} \Leftrightarrow 2\ 5'\ \mathrm{CGTACATGTA}\ 3' \qquad (1)$$

where, 8 of the 10 bases are self-complementary in the reverse direction. Fukada et al.[12] have shown that for a protein oligomer A_m denaturing and dissociating into its identical subunits B,

$$\ln\{[A_m]\} = -\Delta H_{vH}/[RT_p(m-1)] + \text{constant} \qquad (2)$$

So that for ssDNA sequence 5, a plot of the ln of the ssDNA sequence concentration versus the reciprocal of the temperature at the peak maximum, T_p, yields $\Delta H_{vH} = 83 \pm 7$ kJ $mol^{-1}$for $m = 2$, which is within 2 standard deviations of the transition enthalpy of 134 ± 23 kJ mol^{-1}. The factor $m = 2$ would validate that the original state of the ssDNA sequence is that of a dimer. However, all the other ssDNA sequences investigated have only up to 60% of the bases self-complementary in the reverse direction, including the sequences that do not exhibit a transition between 10 and 95°C (Tables II and III). Since many of the ssDNA sequences in Table I were one or two bases self-complementary in the reverse direction, then there is a possibility that the bases, in particular the C or G bases, near the 5′ end would interact with their complementary G and C bases near the 3′end of the ssDNA sequence to form a stem–loop (hairpin) ssDNA conformation. The observed transitions would then be considered hairpin⇔coil transitions and would also be independent of ssDNA concentration.

Early investigations of hairpin⇔coil transitions showed that the thermodynamics of formation was essentially dependent on the complementary bases in the stem and that the contribution of the bases in the loop to the formation of CGAAG(XXXX)CGTTCG, for example, was relatively small, ranging from changes in the transition temperatures of 66.9°C for X = T to 62.6°C for X = A.[13] If ssDNA sequences 8 through 22 in Table I exhibited hairpin⇔coil transitions, then the stems of these ssDNA hairpin conformations would only have 2 complementary CG pairs in the stem with an additional complementary AT pair only in ssDNA sequences 9 and 11 and loops ranging from 2 to 4 bases. However, a hairpin conformation with consistently only 2 complementary CG pairs in the stem can not account for the wide disparity of transition temperatures from 37.1°C for ssDNA sequence 8 to 69.9°C for ssDNA sequence 22. The reported SANS measurements on ssDNA sequence 15 in Table I with 2 complementary CG pairs in the stem of a possible hairpin conformation shows that it does not exist in the hairpin conformation in solution.[4] If a hairpin conformation could be formed by the interaction of only 2 complementary CG pairs in the stem, then the ssDNA sequences 23 through 27 in Table II should also exhibit transitions, but no transitions are observed for these ssDNA sequences. Accordingly, the ssDNA sequence transitions with the exception of the ssDNA sequence 5 transition were considered to be S⇔U transitions and were analyzed in terms of the two-state A⇔B transition model.

Basically, all the S⇔U transitions exhibit transition to van't Hoff transition enthalpy ratios of less than one implying that only part of the stacked nucleotides of a sequence contributes to the transition enthalpy. The van't Hoff enthalpies that are derived from the temperature dependence of the equilibrium distribution between the populations of the stacked and unstacked ssDNA sequence species appear to be independent of chain length from 10 to 12 nucleosides. This has been observed earlier for RNA sequences where the transition van't Hoff enthalpy derived from the UV melting

Table IV Classification of ssDNA Sequences with S⇔U Transitions into T_m Ranges

T_m (°C)	ssDNA Sequence	Sequence Length	Possible Nucleation Quadruplets in Each Sequence	Possible Unique Nucleation Quadruplets
15–25	1	10mer	ACCA, ATGT	ACCA, ATGT
	2	12mer	GCTT, TGTA, TTTG	GCTT, TGTA
	3	10mer	CATG	CATG
	4	10mer	TGTG, TTTG	TGTG
	37	12mer	ATGT, TGTG, GTGG	ATGT, TGTG, GTGG
	42	12mer	ACCA, TACC	ACCA, TACC
30–41	6	12mer	AGCG, GCGT	AGCG, GCGT
	7	10mer	TTTG, TGTA	TGTA
	41	12mer	TACC, ATGG, TGGT	TACC, ATGG, TGGT
	8	10mer	CAGA, GCAG	CAGA, GCAG
	9	11mer	GCGT	GCGT
	10	10mer	CGAT	CGAT
	11	12mer	CAGA, GCAG	CAGA, GCAG
43–49	12	11mer	CTCC, TCCA, CATG	CTCC, TCCA
	13	10mer	GCCC, CCCA, CATG	GCCC, CCCA
	14	10mer	CATA, TAGG, GCAT	CATA, TAGG, GCAT
	15	10mer	GCTG, TGAT	GCTG, TGAT
	16	10mer	CCTA	CCTA
	17	10mer	CATA, TACG, ACGC CGCA, GCAT	CATA, TACG, ACGC CGCA, GCAT
	18	10mer	CATC, TCGG, CGGC, GCAT	CATC, TCGG, CGGC, GCAT
	19	10mer	AAAT, CAAA	AAAT, CAAA
	20	10mer	CATG, ATGT, TGTG, GCAT	GCAT
	21	10mer	GCAT, TTTG	GCAT
70	22	10mer	GCGT	GCGT

curves was independent of chain length in going from the dinucleoside ApA to a longer poly A sequence.[5] If all the bases of the ssDNA sequence contribute to the transition enthalpy then the ratio of the transition enthalpy to the van't Hoff transition enthalpy would be unity. Apparently, only part of the sequence contributes to the S⇔U transition enthalpy with about 10% for the weaker transitions where the transition to van't Hoff enthalpy ratios are less than 0.10 and 35% for the stronger transitions. The weaker transitions tend to occur predominately at lower temperatures as shown in Table I but it is not known as to how the transition temperature depends on sequence. There does not appear to be any correlation between the transition temperature and the number of purine and/or pyrimidine bases in the sequence as well as the number of CG doublets present in the ssDNA sequence.

In Tables I–III, 22 out of the 46 ssDNA sequences investigated, almost 50%, do not exhibit S⇔U transitions in the temperature range from 10 to 95°C. The presence of a transition in this temperature range may depend on the presence of a smaller "nucleation" subsequence initiating the stacked conformation in this temperature range. Would this nucleation sequence be a doublet, triplet, or a quadruplet of nucleosides? The nucleation subsequence is not a specific doublet since the total 46 ssDNA sequences in Tables I—III contain all the possible 16 doublets of the 4 bases of DNA whether or not the ssDNA sequences are transition sequences. All the 64 triplets are present in the 46 ssDNA sequences. Only the ACC triplet in sequence 1, the ACG and CGC triplets in sequence 17, the TCG triplet in sequence 18, and the AAA triplet in sequence 19 are not found in the 21 non-transition sequences. Since all the other triplets are found in both the transition and non-transition ssDNA sequences, a triplet of bases does not seem to be responsible for nucleation of the stacking of the 24 transition ssDNA sequences, excluding sequences 1 and 17–18.

Since the specific 59 triplet sequences could not be classified as nucleation sites, quadruplet sub sequences were considered as a possible nucleation sites and, thus, the 46 ssDNA sequences were divided into quadruplet sub sequences. However, there are a total of 256 quadruplets of the four bases and only 141 are present in the 46 ssDNA sequences in Tables I–III. Of the total 46 ssDNA sequences investigated, 105 quadruplets are found in the non transition ssDNA sequences and the remaining 36 quadruplets in the transition ssDNA sequences. Each of the transition ssDNA sequences

contains one or more of the 36 quadruplets not found in the non transition ssDNA sequences and, thus, these specific 36 quadruplets may be considered as possible nucleation sequences for the stacking process. It should be emphasized that only 141 out of a possible 256 quadruplets were sampled in this investigation. It is quite possible that other ssDNA sequences containing any of the remaining uninvestigated 115 quadruplets may exhibit a S⇔U transition between 10 and 95°C and yet not contain a quadruplet other than those found in the non transition ssDNA sequences. This would then rule out a quadruplet as the exclusive nucleation site. Perhaps the transition temperature and enthalpy can be attributed to the sequence of the nucleation quadruplets since only a portion of the bases of an ssDNA sequence appear to contribute to the transition enthalpy.

In an attempt to correlate the thermal stability of the stacking conformation in terms of the S⇔U transition temperature with the nucleation quadruplet, the 24 ssDNA sequences exhibiting an S⇔U transition are separated into four conformational stability classes according to their transition temperatures, 15–25°C, 31–42°C, from 43 to 50°C, and 70°C as shown in Table IV. In Table IV, some quadruplets of the same sequence, however, are found in different temperature stability classes. More specifically, CATG is found in the 15–25°C and the 43–49°C classes, GCGT is found in the 30–41°C and 70°C classes, TGTG is found in the 15–25°C and 43–49°C classes, and TTTG is found in all the classes except the 70°C class. Since TTTG is found in almost all the classes, it may not be considered a nucleation quadruplet. Since CATG and TGTG are found in low and higher temperature classes, they may be considered nucleation quadruplets in only the low temperature class. At higher temperatures they would be too unstable as a nucleation site to initiate stacking of the entire ssDNA sequence.

In fact, CATG and TGTG are the only possible nucleation quadruplets found, respectively, in ssDNA sequence 3 and in ssDNA sequence 4, where both ssDNA sequences are in the 15–25°C class. The length of the ssDNA sequence may also be important in the stacking process since the longer than 10mer sequences, with the exception of ssDNA sequence 9, have at least two possible nucleation quadruplets in their sequences. GCGT is the only possible nucleation quadruplet in the 11mer ssDNA sequence 9 in the 30–41°C class and the 10mer ssDNA sequence 22 in the 70°C class. If the stacking of the bases is inhibited by a longer sequence length, then although nucleation is initiated by the same quadruplet, it may proceed at a lower temperature for a longer sequence as is the case for ssDNA sequence 9. The possible nucleation quadruplets unique in each temperature stability class are now listed in the last column of Table IV. It may well be that other factors have to be considered in determining the thermal stability of the stacking process. For example, the role of the backbone conformation in the thermal stability has been implicated in earlier Laser Raman spectra studies of doublet, triplet, and long chain ribonucleotides.[14] Laser Raman spectra of poly(rA) and poly(rC) confirm their stacked conformations but suggest that the backbone conformation in the more thermally stable poly(rC) differs from that of most stacked structures.[14] Furthermore, the directionality of the doublet is important in that UpA is stacked at low temperature, whereas ApU is not stacked and the backbone conformation of ApU differs from that found in UpA.[14] However, based on the ssDNA sequences of this investigation and the restraints just described the stacking of ssDNA sequences may be initiated by a unique nucleation quadruplet site in the sequence.

The effect of salt on the stability arises purely out of entropic effects since the two-state A⇔B transition temperatures change, while the transition enthalpies remain essentially the same for each sequence. More specifically, for a A⇔B transition,

$$\Delta_{\mathrm{trs}} G = 0 \tag{3a}$$

$$\Delta_{\mathrm{trs}} S = \Delta_{\mathrm{trs}} H / T_{\mathrm{m}}. \tag{3b}$$

More specifically, all of the ssDNA sequences exhibit an increase in the transition temperature at 0.1*M* NaCl with the exception of ssDNA sequences 4, 13, 14, 18, 20, 21, and 22. ssDNA sequences 14 and 20 exhibit, however, a decrease in T_{m} at 0.1*M* NaCl, while ssDNA sequences 13, 14, 18, 21, and 22 exhibit no change within experimental error in T_{m}. For the 15 sequences exhibiting a temperature increase at 0.1*M* NaCl concentration in Tables I–III, the transition entropy is reduced upon unstacking of the ssDNA sequence, implying that the NaCl ions either destabilize the final unstacked state of the ssDNA sequence or stabilize the initial stacked state of the sequence. For the two ssDNA sequences exhibiting a temperature decrease with increase in the NaCl concentration, the transition entropy increases, implying that the NaCl ions either destabilize the initial stacked conformation and/or further stabilize the final, unstacked conformation.

In Table III, most of the ssDNA complementary promoter sequences do not undergo an S⇔U transition from 10 to 95°C indicating the lack of the formation of an ssDNA stacking conformation upon separation of the promoter duplex in the transcription bubble. In addition, there is no correlation between the stability of the stacked conformation of each of the five complementary transition ssDNA sequences and the lifetime of the transcription initiation complex. However, this does not necessarily preclude a role for the stacked con-

formation in many other biological processes involving ssDNA.

The authors wish to thank Deidre Carroll and Amy Hapip for their assistance with the experimental measurements. Certain commercial materials, instruments, and equipment are identified in this article to specify the experimental procedure as completely as possible. In no case does such identification imply a recommendation or endorsement by the National Institute of Standards and Technology nor does it imply that the materials, instruments, or equipment identified is necessarily the best available for the purpose.

REFERENCES

1. Warshaw, M. M.; Cantor, C. R. Biopolymers 2004, 9, 1079–1103.
2. Vesnaver, G.; Breslauer, K. J. Proc Natl Acad Sci USA 1991, 88, 3569–3573.
3. Chakrabarti, M. C.; Schwarz, F. P. Nucleic Acids Res 1999, 27, 4801–4806.
4. Zhou, J.; Gregurick, S. K.; Krueger, S.; Schwarz, F. P. Biophys J 2006, 90, 1–8.
5. Leng, M.; Felsenfeld, G. J. Mol Biol 1966, 15, 455–466.
6. Schwarz, F. P.; Robinson, S.; Butler, J. M. Nucleic Acids Res 1999, 27, 4792–4800.
7. Mikulecky, P. J.; Feig, A. L. Biochemistry 2006, 45, 604–616.
8. Jelesarov, I.; Crane-Robinson, C.; Privalov, P. L. J Mol Biol 1999, 294, 981–995.
9. Brunner, M.; Bujard, H. EMBO J 1987, 6, 3139–3144.
10. Kallansrud, G.; Ward, B. Anal Biochem 1996, 236, 134–138.
11. Kirchhoff, W. H. NIST Tech. Note 1401. US Government Printing Office: Washington, DC, 1993, 1–103.
12. Fukada, H.; Sturtevant, J. M.; Quiocho, F. A. J Biol Chem 1983, 258, 13193–13198.
13. Senior, M. M.; Jones, R. A.; Breslauer, K. J. Proc Natl Acd Sci USA 1988, 85, 6242–6246.
14. Prescott, B.; Gamache, J.; Livramento, J.; Thomas, G. J., Jr. Biopolymers 1974, 13, 1821–1845.

Reviewing Editor: Sarah Woodson